RENORMALIZATION-GROUP STUDY OF FIBONACCI CHAINS

D. WÜRTZ [1], T. SCHNEIDER and A. POLITI [2]
IBM Research Division, Zurich Research Laboratory, 8803 Rüschlikon, Switzerland

Received 7 January 1988; accepted for publication 4 March 1988
Communicated by A.R. Bishop

We report an exact renormalization-group treatment for general Fibonacci chains, including the electronic tight-binding, phonon and diffusion problems. Analysis of the fixed points and the cycles yields the scaling properties of the states and spectra. As an example, we treat a lattice dynamic model.

The ability to produce superlattices by adding individual atomic layers [1] is a revolutionary advance, which has generated considerable interest in the studies of physical properties of quasiperiodic systems in one dimension [2–11]. Theoretically, quasiperiodic potentials are interesting because Bloch's theorem is inapplicable. These potentials lead to rich eigenvalue spectra and wave functions because they are intermediate between random and periodic [2–11]. Periodic potentials lead to continuous spectra with gaps and extended eigenstates, while random and uncorrelated potentials exhibit pure-point spectra and exponentially localized states. In this Letter, we report an exact renormalization-group (RG) approach to the study of spectra and wave functions of Fibonacci chains. The approach is based on an exact decimation yielding recursion relations amenable to a fixed-point analysis which governs the scaling properties of states and spectra. Previous attempts either used approximations [5,6] or concentrated on the diagonal tight-binding model [3,4]. In contrast, we consider the general tight-binding model and present the exact recursion relations, yielding, in terms of a fixed-point analysis, the scaling properties of the states and spectra. As a specific example, we treat a lattice dynamic model.

[1] On leave from Institut für Theoretische Physik, Universität Heidelberg, Philosophenweg 19, 6900 Heidelberg, FRG.
[2] On leave from Istituto Nazionale di Ottica, Largo E. Fermi 6, 50125 Florence, Italy.

We consider the general tight-binding hamiltonian

$$t_{n+1,n}\phi_{n+1} + t_{n-1,n}\phi_{n-1} = (V_n - M_n z)\phi_n \,. \qquad (1)$$

In the electronic problem, ϕ_n denotes the wave function at the nth site, $\{t_{n\pm1,n}\}$ and $\{V_n\}$ are Fibonacci sequences of hopping matrix elements and potentials, respectively, while $M_n z \equiv \omega$ denotes the energy. In the phonon problem on the other hand, ϕ_n now describes the displacement of mass M_n from its equilibrium position. The spring constants t, potentials V and masses M form Fibonacci sequences, and $z=\omega^2$ is the frequency of the lattice vibrations. Moreover, eq. (1) can also be interpreted as a discrete imaginary-time Schrödinger problem, resulting from a diffusion equation. The quasiperiodic structure is generated in terms of two different elementary units, according to the Fibonacci inflation rule. The two units consist of two blocks A and B and two bonds, weak (–) and strong (=). Connecting these units =A and –B according to the Fibonacci inflation rule, =A, =A–B, =A–B=A, =A–B=A=A–B, ... and so forth, we identify two different blocks A: One is embedded between two strong bonds, =A=, and the other between a strong and a weak bond, =A–. We distinguish between these two cases because the potential V may depend on the surrounding bonds. Thus, we mark A followed by a weak bond with a tilde $\tilde{\text{A}}$–. If A is the last black in a given sequence, the information whether A is followed by a weak or strong bond, will be obtained from the next inflation. Formally, the sequence can be generated by ap-

0375-9601/88/$ 03.50

plication of the inflation rule $Q_{l+1}=Q_lQ_{l-1}$, starting with units Q_1: A=: S and Q_2: $\tilde{\text{A}}$=: L. The short and long units are denote by S and L, respectively. The generation of the sequence is illustrated in fig. 1a.

The renormalization-group approach can now be invoked by decimating the system of size F_l to a system on the $(l-1)$th inflation level with rescaling factor $\sigma_G(l)=F_l/F_{l-1}$. The F_l's are the Fibonacci numbers $F_{l+1}=F_l+F_{l-1}$ with initial conditions $F_0=F_1=1$; $\sigma_G(l)$ is the lth rational approximant to the golden mean $\sigma_G=\sigma_G(l\to\infty)=(\sqrt{5}+1)/2$. This decimation transformation is identical to the deflation where the blocks LS: $\tilde{\text{A}}$–B=A– go to L': $\tilde{\text{A}}'$–B'= and the remaining long blocks L: $\tilde{\text{A}}$–B go to S': A'=. This deflation, or decimation, scheme is illustrated in fig. 1b. To be more specific, we revert to the tight-binding hamiltonian (1),

$$\begin{pmatrix}\phi_{n+1}\\ \phi_n\end{pmatrix}=\begin{pmatrix}\dfrac{V_n-M_nz}{t_{n+1,n}} & -\dfrac{t_{n-1,n}}{t_{n+1,n}}\\ 1 & 0\end{pmatrix}\begin{pmatrix}\phi_n\\ \phi_{n-1}\end{pmatrix}$$

$$=\mathbf{M}_n\begin{pmatrix}\phi_n\\ \phi_{n-1}\end{pmatrix}. \qquad (2)$$

In terms of blocks L and S, three distinct Schrödinger equations are then obtained:

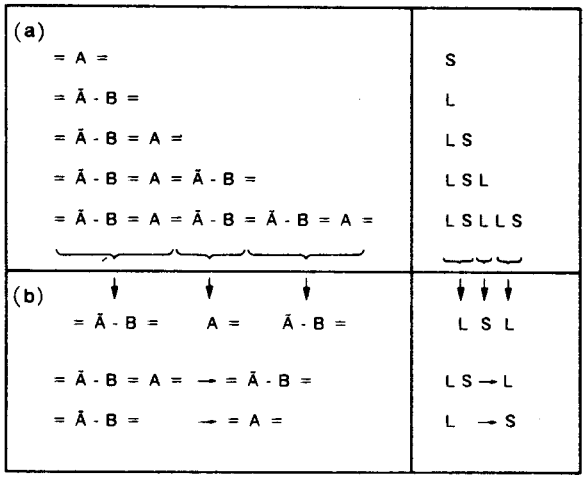

Fig. 1. (a) Inflation, and (b) decimation rules.

$$\text{S:}\quad =\text{A}=:\ \phi_{n+1}+\phi_{n-1}=2x\phi_n,$$

$$\text{L:}=\text{A–B}=\begin{cases}=\text{A}–:\ \phi_{n+1}+\dfrac{1}{r}\phi_{n-1}=2y\phi_n,\\ \text{–B}=:\ \phi_{n+1}+r\phi_{n-1}=2z\phi_n,\end{cases} \qquad (3)$$

where r is the ratio between the weak (–) and strong (=) bonds, while the quantities (x, y, z) measure local properties,

$$r=s/d,\quad x,y,z=(V_{\text{A},\tilde{\text{A}},\text{B}}-M_{\text{A},\tilde{\text{A}},\text{B}}z)^{1/2}. \qquad (4)$$

Next, we implement the decimation from F_l to F_{l-1}. In doing so, the three elementary sequences depicted in fig. 1b must be distinguished and decimated according to the rules given there. Then invoking eqs. (2), (3) and (4), we obtain the recursion relations

$$r'=2y,\quad x'=2yz-r/2-1/2r,$$
$$y'=z-r/4y,\quad z'=2xy-1/2r. \qquad (5)$$

These recursion relations can be interpreted as follows: Given an eigenstate of a system of size F_{l+1}, there exists a corresponding solution with parameters (r', x', y', z') on a lattice with F_l sites. Accordingly, we can rewrite the recursion relations in the discrete form

$$r_{l+1}=2y_l,\quad x_{l+1}=2y_lz_l-r_l/2-1/2r_l,$$
$$y_{l+1}=z_l-r_l/4y_l,\quad z_{l+1}=2x_ly_l-1/2r_l. \qquad (6)$$

It is also useful to express parameters r, x, y, and z in terms of the transfer matrices $\mathbf{M}^{l-1}$ and $\mathbf{M}^l$, where

$$\mathbf{M}^l=\prod_{F_l}^{n=1}\mathbf{M}_n. \qquad (7)$$

This yields

$$r_l=M^l_{21}/M^{l-1}_{21},$$
$$x_l=\tfrac{1}{2}(M^l_{11}+M^l_{22})=\tfrac{1}{2}\,\mathrm{Tr}\,\mathbf{M}^l,$$
$$y_l=\frac{1}{2}\left(M^{l-1}_{22}+\frac{1}{r_l}M^l_{11}\right),$$
$$z_l=\tfrac{1}{2}(M^l_{22}+r_lM^{l-1}_{11}).$$

Introducing new variables $u_l=y_l-(x_l-z_l)/r_l$ and $w_l=r_ly_l-x_l$, it is easily verified that trace x_l satisfies

the well-known trace recursion relation [3,4]

$$x_{l+1}=2x_l x_{l-1}-x_{l-2}\,, \tag{9}$$

with invariant

$$I=x_{l-1}^2+x_l^2+x_{l+1}^2-2x_{l-1}x_l x_{l+1}-1\,. \tag{10}$$

Previously, trace map (9) played a crucial role in determining the energies belonging to the spectrum [3,4,9,10]. In fact, if $|x_l|$ remains bounded (cyclic or aperiodic), the energy will belong to the spectrum, while unbounded $|x_l|$'s characterize gap states. Moreover, the cycles are amenable to a fixed-point analysis, allowing elucidation of certain scaling properties of the spectrum. The important role of the trace in determining the energy spectrum can be understood from the fact that for systems subjected to periodic or antiperiodic boundary conditions and energies belonging to the spectrum, the trace satisfies $|x_l|<1$. In this context, it is important to recognize that recursion relations (6) are more general. In fact, from eq. (8) it is seen that for given initial values, say $M_{11}^{0,1}$, $M_{22}^{0,1}$ and $M_{21}^{0,1}$, iteration of the recursion relations determines M_{11}^{l}, M_{22}^{l} and M_{21}^{l}. The fourth matrix element follows from the unimodularity of the transfer matrix on the Fibonacci sublattice: $\det \mathbf{M}^l=1$. Accordingly, the RG-recursion relations fix all elements of the transfer matrix for given initial conditions. This opens up the possibility of analyzing not only the energy spectrum but also the properties of the wave functions with the RG approach.

As an example, we consider the lattice dynamic model

$$u_{n+1}+u_{n-1}=(2-M_n\omega^2)u_n\,, \tag{11}$$

to illustrate the application of the RG approach outlined above. We assume two kinds of masses M_A and M_B arranged according to the Fibonacci inflation rule: A, AB, ABA, ABAAB, ... Numerical results for the integrated density of states $N(\omega)$ and the exponential growth rate $\gamma(\omega)$, as obtained from the recursion relation

$$R_{n+1}=2-M_n\omega^2-1/R_n\,,\quad R_n=u_n/u_{n-1} \tag{12}$$

in terms of node counting, for $M_A=1$ and $M_B=3$ are shown in fig. 2. $N(\omega)$ grows linearly for small ω, and becomes more fragmented with increasing ω. This behvior is consistent with the ω dependence of invariant (10) given by

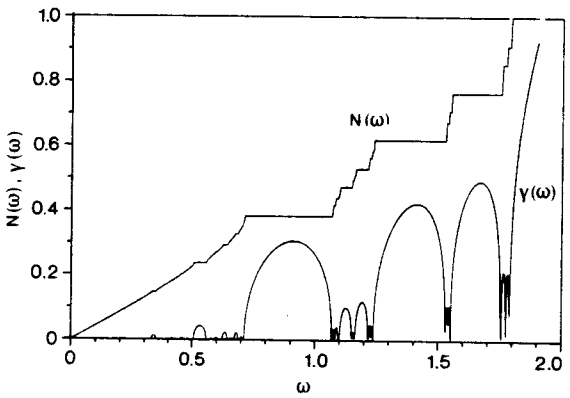

Fig. 2. Integrated density of states $N(\omega)$ and exponential growth rate $\gamma(\omega)$ versus frequeny ω for the lattice dynamic model with masses $M_A=1$ and $M_B=3$.

$$I=\tfrac{1}{4}(M_A-M_B)^2\omega^4\,, \tag{13}$$

because

$$x_{-1}=1\,,\quad x_0=\tfrac{1}{2}(2-M_B\omega^2)\,,$$
$$x_1=\tfrac{1}{2}(2-M_A\omega^2)\,. \tag{14}$$

In fact, the fragmentation in $N(\omega)$ increases with increasing $I(\omega)$. We also note that gaps can be labeled by two integers, m and n. The integrated density of states $N(m, n)$ below gap m, n is then given by $0\leqslant n+m\sigma_G\leqslant 1$. To elucidate the linear ω dependence in the limit $\omega\to 0$, we note that for $\omega=0$ recursion relations (6) and trace map (9) exhibit a fixed point with

$$x^*=1\,,\quad y^*=\tfrac{1}{2}\sigma_G\,,$$
$$z^*=\sigma_G-1/2\sigma_G\,,\quad r^*=\sigma_G\,. \tag{15}$$

Linearization of trace map (9) around the fixed point yields the three eigenvalues $\lambda_1=-1$, $\lambda_2\equiv\lambda=\sigma_G^2$ and $\lambda_3=1/\lambda$. For energies $\omega^*+\Delta\omega$, where ω^* leads to the fixed point, scaling then implies

$$|N((\omega^*+\Delta\omega)^2)-N((\omega^*)^2)|\sim(\Delta\omega)^{2\delta}\,,$$

$$\bar{x}=\frac{\ln \sigma_G}{|\ln|\lambda||}\,, \tag{16}$$

Thus, scaling yields $N(\omega^2)\sim\omega$, confirming the linear behavior seen in fig. 2.

Because the ground state with frequency $\omega=0$ is extended, the leading term of $N(\omega^2)$ can be calculated exactly. Following ref. [12], we find

$$N(\omega^2)=\frac{1}{\pi}\omega\langle M\rangle^{1/2}\,,$$

$$\langle M\rangle=\frac{1}{\sigma_G}M_A+\left(1-\frac{1}{\sigma_G}\right)M_B\,. \tag{17}$$

In addition to this homogeneous fixed-point behavior for $\omega=0$, there are many other energies in the spectrum, where recursion relations (6) and trace map (9) exhibit cyclic or aperiodic bounded iterates. The fragmented, Cantor-set-like structure of the integrated density of states $N(\omega)$ implies, however, that these energies do have measure zero. An example is $\omega=0.5048147789047881...$, yielding the six-cycle (a, −b, −a, b, −a, −b) in trace map (9). This cycle is depicted in fig. 3, together with the associated six-cycle appearing in the variables of the RG-recursion relations (6). On this basis, the properties of the wave function are now readily deduced. Invoking the boundary condition $\phi_0=0$, eqs. (6) and (8) yield

$$\phi_{F_l}=\prod_{j=1}^{l} r_j\sim(\alpha\beta)^{3n}=(\alpha\beta)^{l/2}\,, \tag{18}$$

where $(\alpha, -\beta, -\alpha, \beta, -\alpha, -\beta)$ denote the elements of the six-cycle in iterates r_l, and $n=l/6$ is the number of cycles. A plot of $\ln|\phi_{F_l}|$ versus l, as obtained from the RG-recursion relations is shown in fig. 4a, yielding the slope $\ln(\alpha\beta)^{1/2}\sim 0.49$. Because F_l and cycle $\{r\}_l$ scale as $F_{l+6}\to\sigma_G^6 F_l$ and $\{r\}_{l+6}\to(\alpha\beta)^3\{r\}_l$, respectively, we obtain $\phi_{F_l}\sim(F_l)^{\bar{y}}$, with $\bar{y}=3\ln(\alpha\beta)/6\ln\sigma_G\sim 1.02$, as shown in fig. 4b. Comparison with wave function $|\phi_n|$ indicates that on the real lattice scaling is governed by a distribution of exponents [12] with an average close to the exponent on the Fibonacci sublattice.

Finally, we turn to the scaling properties of the integrated density of states $N(\omega)$, which are fully determined by trace map (9). Assuming an initial frequency ω^*, which under iterations yields a cycle

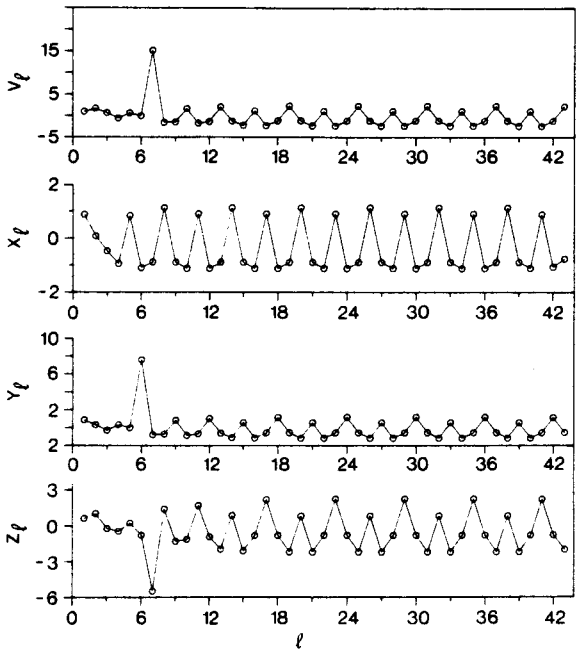

Fig. 3. Iterates r_l, x_l, y_l and z_l of the RG-recursion relation for $\omega=0.5048...$, and $M_A=1$, $M_B=3$ yielding a six-cycle.

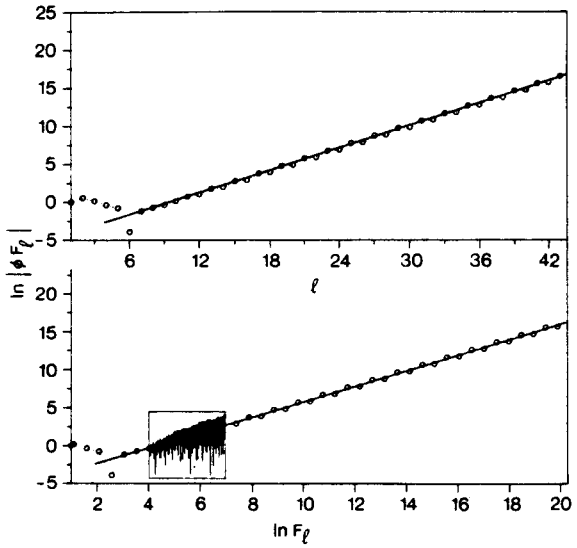

Fig. 4. Scaling behavior of the wave function for $\omega=0.5058...$, and $M_A=1$, $M_B=3$ yielding a six-cycle. (a) $\ln|\phi_{F_l}|$ versus l; (b) $\ln|\phi_{F_l}|$ versus $\ln F_l$, and in the insert $\ln|\phi_n|$ versus $\ln n$ on the real lattice.

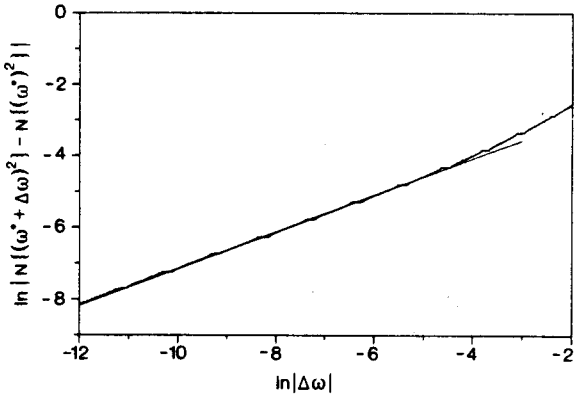

Fig. 5. Scaling of the integrated density of states $N(\omega)$ around the six-cycle with $\omega=0.5048...$, and $M_A=1$, $M_B=3$. The straight line corresponds to the slope 0.51.

of period six, scaling predicts, in close analogy to eq. (16),

$$|N((\omega^*\pm\Delta\omega)^2)-N((\omega^*)^2)| \sim (\Delta\omega)^{2\bar{x}}G\left(\frac{6\ln|\Delta\omega|}{\ln|\lambda|_{\max}}\right),$$

$$\bar{x}=\frac{6\ln\sigma_G}{\ln|\lambda|_{\max}}. \qquad (19)$$

Amplitude G is periodic. The argument is the ratio between $\ln|\Delta\omega|$ and $\Delta/2\bar{x}$, where $2\bar{x}$ is the slope and $\Delta=\ln\sigma_G$ the spacing between major gaps on a logarithmic scale. $|\lambda|_{\max}$ denotes the largest eigenvalue of the trace map, linearized around the cycle. For the six-cycle depicted in fig. 3, we find $|\lambda|_{\max}\sim(6.951)^3$, yielding with eq. (19) $2\bar{x}\sim 0.50$. These scaling predictions are nicely confirmed by the numerical results depicted in fig. 5, including the period of amplitude G, $p=\frac{1}{6}\ln|\lambda|_{\max}\approx 0.97$.

In this Letter, we have presented an exact renormalization-group approach to general Fibonacci chains, yielding the scaling properties of states and spectra from the fixed-point analysis of the recursion relations. Recognizing that a veriety of physical systems can be reduced to the tight-binding form given by eq. (1) including the continuous Krönig–Penney model [13] and light propagation in multilayers [10,14], our exact RG treatment will have a wide range of applications. Moreover, it provides a sound basis for determining the global scaling properties [11].

We thank F. Rys for useful discussions.

References

[1] J.P. Chadi, W.A. Harrison and R.Z. Bachrach, eds., Proc. 17th Int. Conf. on Physics of semiconductors (Springer, Berlin, 1985).
[2] R. Merlin, K. Bajema, F.Y. Juang and P.K. Bhattacharaya, Phys. Rev. Lett. 55 (1985) 1788.
[3] M. Kohomoto, L.P. Kadanoff and C. Tang, Phys. Rev. Lett. 50 (1983) 1870.
[4] S. Ostlund, R. Pandit, D. Rand, H.J. Schnellnhuber and E.D. Siggia, Phys. Rev. Lett. 50 (1983) 1873.
[5] Q. Niu and F. Nori, Phys. Rev. Lett. 57 (1986) 2057.
[6] F. Nori and J.P. Rodriguez, Phys. Rev. B 34 (1986) 2207.
[7] P. Hawrelak and J.J. Quinn, Phys. Rev. Lett. 57 (1986) 380.
[8] J.A. Verges, L. Brey, E. Louis and C. Tejedor, Phys. Rev. B 35 (1987) 5770.
[9] T. Schneider, A. Politi and D. Würtz, Z. Phys. B 66 (1987) 469.
[10] M. Kohomoto, B. Sutherland and K. Iguchi, Phys. Rev. Lett. 58 (1987) 2436.
[11] W.M. Zheng, Phys. Rev. A 35 (1987) 1467.
[12] T. Schneider, M.P. Soerensen, A. Politi and M. Zanetti, Phys. Rev. Lett. 56 (1986) 2341.
[13] D. Würtz, M.P. Soerensen and T. Schneider, unpublished.
[14] D. Würtz, T. Schneider and M.P. Soerensen, unpublished.